Vaccinia DNA Topoisomerase I: Single-Turnover and Steady-State Kinetic Analysis of the DNA Strand Cleavage and Ligation Reactions†

James T. Stivers,‡,§ Stewart Shuman,‖ and Albert S. Mildvan*,‡

Department of Biological Chemistry, The Johns Hopkins School of Medicine, 725 North Wolfe Street, Baltimore, Maryland 21205, and Program in Molecular Biology, Sloan-Kettering Institute, New York, New York 10021

Received August 25, 1993; Revised Manuscript Received October 15, 1993⊛

ABSTRACT: Vaccinia DNA topoisomerase I catalyzes a reversible, site-specific strand cleavage and resealing reaction with duplex DNA involving a transient 3′-phosphotyrosyl linkage between the DNA and Tyr-274 of the enzyme. Single-turnover and steady-state kinetic measurements, as well as DNA binding studies with DNA duplexes containing the preferred cleavage sequence (5′-CCCTT↓-3′) in 50 mM Tris-HCl, pH 7.5, at 20 °C, have permitted the evaluation of the individual rate constants for strand cleavage (k_{cl}) and religation (k_r) and for duplex DNA binding and dissociation. The values of k_{cl} = 0.07 s^{-1} and k_r = 0.66 s^{-1} indicate that the internal cleavage equilibrium ($K_{cl} = k_{cl}/k_r = 0.1$) favors the uncleaved E·DNA complex. The apparent second-order rate constant k_{cl}/K_m^{DNA} = 8 × 10^5 M^{-1} s^{-1} for the single-turnover cleavage reaction is 10^2–10^3-fold less than the rate of diffusional encounter and provides an estimate of k_{on} (DNA). Single-turnover cleavage experiments using a duplex substrate with a nonbridging racemic phosphorothioate nucleotide substitution at the cleavage site showed biphasic cleavage kinetics with equal amplitudes for each phase, which was fit to a double exponential: k_{fast} = 0.01 s^{-1} and k_{slow} = 0.0004 s^{-1}. These "thio effects" (= $k_{cl}^{phos}/k_{cl}^{thio}$) of 4.6- and 115-fold indicate that cleavage is at least partially rate-limiting in the single-turnover reaction; the two kinetic phases indicate a strong preference for cleavage of one thio isomer. Multiple-turnover cleavage–religation reactions showed an initial pre-steady-state burst proportional to enzyme, followed by a slower steady-state rate with a value of k_{cat} = 0.006 s^{-1}. The phosphorothioate substrate showed a smaller burst and no significant thio effect on k_{cat}. These results indicate fast chemical steps and largely rate-limiting dissociation of the religated product (K_D = 54 nM) in the steady-state, a conclusion confirmed by direct measurement of the rate constant for product dissociation as 0.01 s^{-1}. $MgCl_2$ (5 mM) increases this rate constant by an order of magnitude, thus explaining the divalent cation induced acceleration of DNA supercoil relaxation by this enzyme. No divalent cation binding by the enzyme was detected indicating this effect to result from metal binding to DNA. The rate constants k_{cl} and k_r for the nucleophilic attack of Tyr-274 and deoxyribose 5′-OH at phosphorus represent ~10^9- and 10^{12}-fold enhancements over the analogous attack of phenolate and alcoholate anions at the phosphorus backbone of DNA in solution at pH 7.5. Consistent with this estimate, the Y274F mutant is at least 10^6-fold less active in cleavage than the wild-type enzyme.

Eukaryotic type I DNA topoisomerases alter the topological state of duplex DNA by transiently cleaving and rejoining one DNA strand during each catalytic cycle (Champoux, 1990). It appears that the cellular function of these enzymes is to provide temporary "swivels" to relax supercoiled DNA which would otherwise accumulate during various genetic processes (Wang, 1985; Kornberg & Baker, 1992). Despite the fact that topoisomerases have been studied intensively for over 20 years and have been shown to play essential roles *in vivo* (Shuman et al., 1989a; Lee et al., 1993), surprisingly little is known about the kinetic properties of these enzymes.

An understanding of the mechanism of the reactions catalyzed by the eukaryotic type I enzymes requires a detailed kinetic analysis. Because of its small size (32 kDa) and sequence-specific interaction with DNA, Vaccinia virus DNA topoisomerase provides an attractive model system for a detailed kinetic analysis of a eukaryotic type I enzyme (Shuman & Moss, 1987; Shaffer & Traktman, 1987). The DNA relaxation reaction catalyzed by this enzyme (Figure 1A) is comprised of a minimum of three steps involving (1) nucleophilic attack by the hydroxyl group of Tyr-274 at the 3′-phosphorus atom of the preferred oligonucleotide cleavage sequence 5′-(C/T)CCTT↓ resulting in covalent attachment of the DNA to the enzyme by a 3′-phosphotyrosyl linkage (Shuman et al., 1989b; Shuman & Prescott, 1990), (2) a topoisomerization step, entailing either strand passage or free rotation, and (3) a strand religation step which reseals the single strand break in the DNA and is likely the microscopic reverse of the first step (Figure 1A). The cleavage and religation steps are freely reversible as evidenced by the religation of the leaving strand or of other DNA strands to the covalent enzyme–DNA complex (Shuman, 1992). The latter reaction demonstrates how this topoisomerase can catalyze DNA strand transfer and suggests a role for the enzyme in genetic recombination (Shuman, 1989, 1991b).

In this paper we describe a detailed kinetic analysis of substrate binding, site-specific DNA strand cleavage and religation, and product dissociation from the Vaccinia enzyme. In these experiments, small oligonucleotide substrates are used which contain the preferred binding and cleavage sequence 5′-CCCTT↓, thereby allowing kinetic studies of the cleavage

† This work supported by grants from the National Institutes of Health to A.S.M. (DK28616) and to S.S. (GM46330).

* To whom correspondence should be addressed.
‡ The Johns Hopkins School of Medicine.
§ American Cancer Society Postdoctoral Fellow.
‖ Sloan-Kettering Institute.

⊛ Abstract published in *Advance ACS Abstracts,* December 15, 1993.

0006-2960/94/0433-327$04.50/0

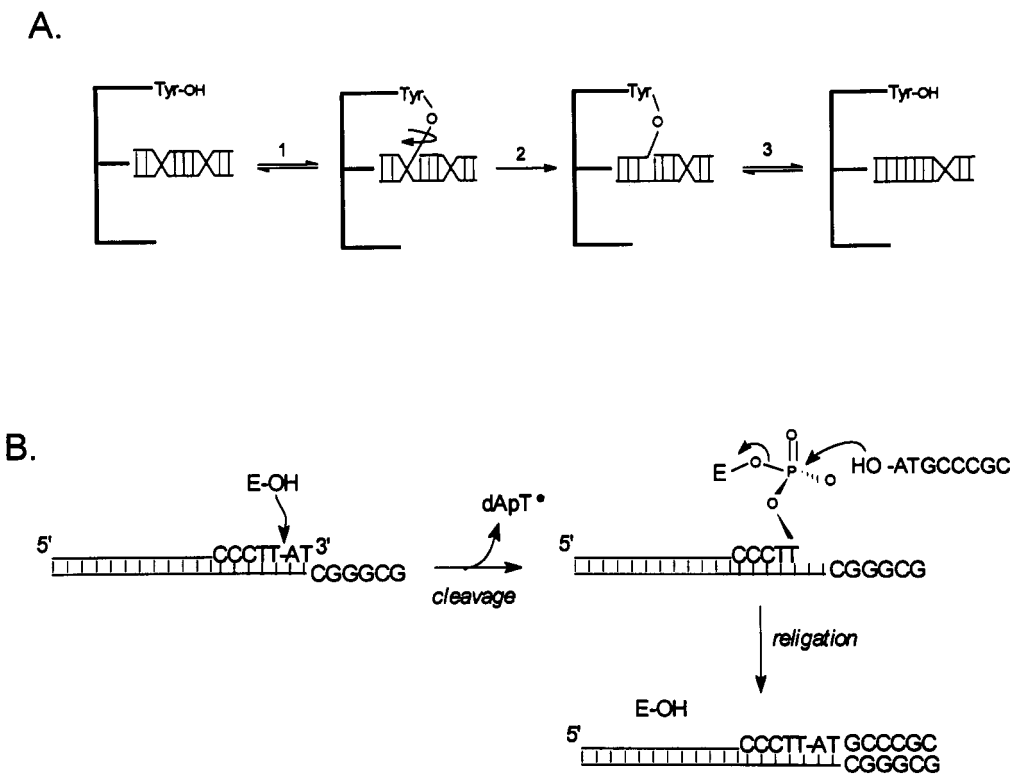

FIGURE 1: (A) Hypothetical mechanism of topoisomerase I catalyzed relaxation of enzyme-bound supercoiled DNA showing the three minimal steps of cleavage, supercoil relaxation, and strand religation. The supercoil relaxation step is arbitrarily shown as involving phosphotyrosine motion. (B) Reaction of Vaccinia enzyme with "suicide" cleavage substrate. Cleavage at the preferred site produces the radiolabeled dinucleotide (dApT*) which irreversibly dissociates from the enzyme. When the cleavage reaction is performed in the presence of a 5'-OH acceptor DNA strand, which is complementary to the single-strand overhang of the cleavage substrate, a religation reaction occurs which releases the enzyme from the cleaved complex to perform multiple cleavage–religation cycles.

and intermolecular religation reactions at a specific site (Figure 1B). Additionally, the availability of "suicide" cleavage substrates, that is duplex oligonucleotides in which the leaving strand is ≤6 nucleotides and irreversibly dissociates from the covalent enzyme–DNA complex (Shuman, 1991a), has provided a method for studying the cleavage and religation reactions under irreversible, single-turnover conditions. The results of these studies have revealed the microscopic rate constants for substrate binding, cleavage, religation, and product release as well as the rate-limiting steps in the steady-state turnover of this enzyme.

MATERIALS AND METHODS

Materials. Radionucleotides [γ-^{32}P]dATP, [α-^{32}P]dTTP, and [methyl-1',2'-^{3}H]dTTP were from New England Nuclear. All unlabeled dNTPs of the highest possible purity were obtained from Pharmacia. Oligonucleotides (phosphodiester and phosphorothioate) were synthesized on an Applied Biosystems 380B DNA synthesizer and purified by reverse-phase HPLC. The sulfurizing reagent, 3H-1,2-benzodithiole-3-one-1,1-dioxide, was from Glen Research, Sterling, VA. Oligonucleotide concentrations were determined by ultraviolet absorbance at 260 nm using the extinction coefficients for the substituent nucleotides (Maniatis et al., 1982).

Enzyme Purification. Wild-type Vaccinia topoisomerase was overexpressed in *Escherichia coli* and purified to >95% homogeneity as judged by a Coomassie Blue R-250 stained SDS–polyacrylamide gel.[1] Purification was essentially as described (Shuman et al., 1988; Morham & Shuman, 1992). Topoisomerase concentrations were determined using the BCA reagent (Pierce) using bovine serum albumin as the standard. The final specific activity of the purified enzyme was 3×10^7 units/mg, where 1 unit is the amount of enzyme required to fully relax 0.2 μg of negatively supercoiled pBR322 DNA in a 20-μL reaction in 15 min at 37 °C and pH 7.5 (50 mM Tris-HCl, 100 mM NaCl, 5 mM $MgCl_2$). The Y274F mutant topoisomerase enzyme was purified through the phosphocellulose chromatography step to >95% homogeneity as judged by a Coomassie Blue R-250 stained SDS–polyacrylamide gel. T4 polynucleotide kinase was from Pharmacia. 3',5'-exonuclease deficient Klenow DNA polymerase was from U.S. Biochemical Corp.

5'-^{32}P-End Labeling of Oligonucleotide Substrates. Synthetic DNA oligonucleotides containing the 5'-CCCTT-3' cleavage motif were labeled at the 5'-end by enzymatic phosphorylation in the presence of [γ-^{32}P]ATP and T4 polynucleotide kinase. Labeled DNA was purified by centrifugal gel filtration through two NICK-Spin columns (Pharmacia) and hybridized in 50 mM Tris-HCl, pH 7.5, to a complementary strand (present at 2-fold molar excess) essentially as described (Shuman, 1991a). The duplex DNAs and oligonucleotides used in these experiments are shown in Figure 2. The percent label incorporation and specific activity of the 5'- and 3'-labeled substrates ($\sim 2 \times 10^6$ cpm/pmol) was determined by thin layer chromatographic (TLC) separation of the unreacted nucleotide and product using Whatman poly(ethylenimine)-cellulose TLC (PEI-TLC) plates essentially as described (Maniatis et al., 1982) except the plates were developed with 0.3 M potassium phosphate, pH 8.0.

[1] Abbreviations: SDS, sodium dodecyl sulfate; Tris, tris(hydroxymethyl)aminomethane; BCA, bicinchoninic acid, sodium salt; HPLC, high-performance liquid chromatography; EDTA, (ethylenedinitrilo)tetraacetic acid, disodium salt; PAGE, polyacrylamide gel electrophoresis.

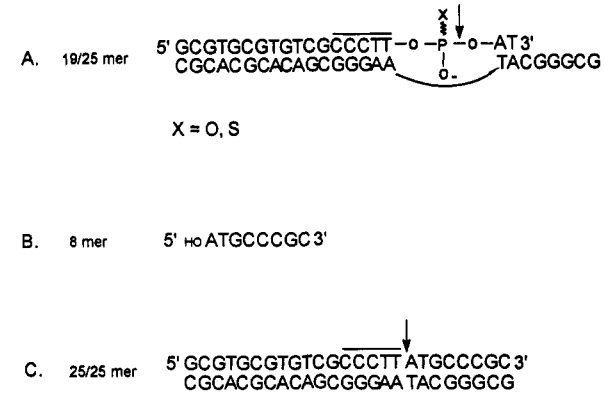

FIGURE 2: DNA substrates used in the experiments. The preferred cleavage site (↓) and pentameric binding motif (—) are indicated. (A) 19/25-mer used in the cleavage experiments. Cleavage at the indicated position (↓) produces the radiolabeled dinucleotide product dApT*, which can be resolved from uncleaved 19*/25-mer by TLC. (B) 5'-HO-8-mer acceptor strand used in the ligation experiments. This sequence is complementary to the eight-nucleotide single-strand overhang produced by cleavage of the 19/25-mer. (C) 25/25-mer product of the coupled cleavage–ligation reactions.

3' Labeling of Substrate Duplexes. The 19/25-mer cleavage substrate 3'-^{32}P-labeled on the cleaved 19-mer strand was prepared from the unlabeled 18/25-mer duplex shown below by incubating 5 μM 18/25-mer, 20 units of Klenow

```
          (5')                (3')
18/25 mer      GCGTGCGTGTCGCCCTTA
               CGCACGCACAGCGGGAATACGGGCG
```

DNA polymerase (exo$^-$), 8 μM [α-^{32}P]dTTP (~3 × 10^6 dpm/pmol), and buffer consisting of 10 mM Tris-acetate, 10 mM magnesium acetate, and 50 mM potassium acetate, pH 7.6, for 30 min at 25 °C in a total volume of 20 μL. An additional 4 μM unlabeled dTTP (2 μL of a 40 μM dTTP solution) was then added and the incubation continued for 15 min. The reaction was quenched with 2 μL of 0.5 M EDTA and then phenol-chloroform extracted and purified as described above for the 5'-labeled oligonucleotides. The 3'-^{32}P-labeled 19*/25-mer substrate with a single phosphorothioate linkage at the cleavage site was prepared similarly except that the phosphodiester 18/25-mer was replaced with the specifically substituted 18/25-mer phosphorothioate analogue, and 1 mM dithiothreitol (DTT) was included in the reaction. The 3'-^{3}H-labeled 19/20-mer substrate was prepared as described above for the 3'-^{32}P-labeled phosphodiester substrate except the reaction contained 0.125 mM [methyl-1',2'-^{3}H]dTTP (~2 × 10^6 dpm/pmol) and 0.033 mM duplex.

Strand Cleavage. Single-turnover cleavage experiments were performed at 20 °C in 50 mM Tris-HCl, pH 7.5, with excess topoisomerase (20–500 nM) and limiting amounts (2–75 nM) of the 3'-labeled 19/25-mer "suicide" substrate (Figure 2A). Under these conditions dissociation of the dinucleotide precludes religation. Cleavage reactions performed on the Kintek rapid-quench apparatus (Johnson, 1986) were initiated by mixing equal volumes (40 μL) of 19/25-mer and enzyme solutions. At time points between 0.50 and 300 s, the reaction was quenched with 2% SDS delivered from the quench syringe; if necessary, an additional amount of 1% SDS was added to the quenched samples to bring the total volume to 280 μL. In the enzyme concentration range 20–200 nM the cleavage reactions (100 μL) with 2 nM 3'-labeled 19/25-mer were mixed and quenched manually (5–9 time points between 5 and 600 s). In these reactions 10-μL time points were quenched in 10 μL of 2% SDS. Unreacted 19*/25-mer substrate was then resolved from the radiolabeled dinucleotide cleavage product (dApT) by spotting 0.5–1 μL of the quenched reaction on a Whatman poly(ethylenimine)-cellulose TLC (PEI-TLC) plate which was then developed with 0.3 M potassium phosphate, pH 8.0. After autoradiographic exposure of the developed plates using Kodak XAR film, the sections corresponding to substrate and product were excised and mixed with 5 mL of EcoLite(+) scintillation cocktail. Their ratio at each time point was quantitated by liquid scintillation spectrometry using a Beckman LS-6000 scintillation counter.

While single-turnover cleavage reactions were first-order for ~3 half-lives, complete conversion of 3'-labeled 19*/25-mer dApT* product was not observed, with typical end point values over the course of this study ranging between 60% and 85%. This incomplete conversion is attributed to an unreactive form of the duplex substrate and not the enzyme because variable end points were seen with different batches of 3'- or 5'-labeled substrate using the same preparation of enzyme. That the incomplete conversion of substrate to product might represent approach-to-equilibrium (reversible) kinetics is inconsistent with the following observations: (1) cleavage reactions carried out under identical conditions on different days gave identical k_{obsd} values even though the end points of the reactions differed by as much as 30%; the observed rate constant for a reversible reaction *decreases* (i.e., the equilibrium becomes more favorable) as the end point increases (Jencks, 1969), and (2) inclusion in the cleavage reaction of a large molar excess of unlabeled 8-mer single-strand DNA, which is complementary to the single strand overhang of the cleaved 19/25-mer substrate, had no effect on the amount of dinucleotide produced in a single-turnover (see Figure 2 and religation kinetics below). If an equilibrium had existed between enzyme-bound and free dinucleotide product, the presence of the unlabeled 8-mer would be expected to efficiently trap the covalent topoisomerase–DNA complex and prevent reassociation of the dinucleotide product resulting in an increase in the cleavage efficiency, which was not observed.

The above observations are consistent with *irreversible* strand cleavage of the 19/25-mer; therefore, the fractional extent of cleavage at the preferred site at each time [$frac_t$ = $(dApT_{cpm})_t/(\text{total cpm})_t$] was normalized to the final observed end point [i.e., $\%_{norm} = (frac_t/frac_\infty) \times 100$].

Strand Religation. The rate of 8-mer strand ligation to the 5'-^{32}P-labeled enzyme–17*/25-mer covalent complex (E–17/25-mer) was determined by single-turnover approach to equilibrium. Under these conditions the observed rate constant for ligation (k_{obsd}) is equal to the sum of the forward rate constant for religation (k_r) and the reverse strand cleavage rate constant (k_{cl}) (Jencks, 1969). The E–17*/25-mer complex was formed by incubating 1 μM topoisomerase with 50 nM 5'-^{32}P-labeled 19*/25-mer in 50 mM Tris-HCl, pH 7.5, for 15–30 min at room temperature. After this incubation 73% (36 nM) of the input DNA was covalently bound to the enzyme as judged by electrophoretic analysis. Forty microliters of the preformed covalent complex was then mixed with 40 μL of 36 μM 8-mer (in 50 mM Tris-HCl, pH 7.5, 20 °C) in the rapid quench flow apparatus. For this experiment the step motor speed was decreased to 40 rpm. Samples at various times (0.5–15 s) were quenched as described above for the rapid quench flow cleavage experiments. The radiolabeled E–17*/25-mer was resolved from free DNA by electrophoresis on a 13% SDS–polyacrylamide gel at 200 V for 2–4 h, and the radioactivity present in the complex and free DNA at each time was determined by liquid scintillation counting of

the excised gel slices. The percent covalent complex remaining at each time was calculated by dividing the radioactivity present in the complex by the total amount of radioactivity [i.e., % covalent complex remaining = (cpm in complex)$_t$/(total cpm)$_t$ × 100].

The first-order rate constant for approach to equilibrium (k_{obsd}, eq 1) was obtained from a nonlinear least-squares fit of the data to a single exponential; the rate constant for religation (k_r) was calculated from k_{obsd} and the measured equilibrium end point for the reaction (K_{cl}) by the simultaneous solution of eqs 1 and 2.

$$k_{obsd} = k_{cl} + k_r \quad (1)$$

$$K_{cl} = k_{cl}/k_r \quad (2)$$

Coupled Cleavage–Religation. The first-order rate constants for the coupled cleavage–religation reaction (Figure 1B) were determined using single-turnover conditions as follows. A mixture consisting of 50 nM 5′-^{32}P-labeled 19/25-mer and 36 μM complementary 8-mer in 50 mM Tris-HCl, pH 7.5, was preincubated for 5 min at 20 °C. Ten 20-μL portions of this mixture were then aliquoted into wells of a 96-well microtiter plate. The ten reactions were initiated by the addition of 20 μL of a 1 μM solution of topoisomerase (50 mM Tris-HCl, pH 7.5). At time points between 2 and 60 s, reaction aliquots (20 μL) were removed and manually quenched in 20 μL of 2% SDS. The amount of substrate 19/25-mer, product 25/25-mer, and covalent E-17/25-mer intermediate at each time point were determined as follows. A 9-μL aliquot of each quenched time point was adjusted to 38% formamide, 0.05% xylene cyanol, and 0.05% bromophenol blue, heated for 4 min at 95 °C, and applied (16 μL) to a 19% polyacrylamide/7 M urea gel. The 5′-^{32}P-labeled 19-mer substrate and 25-mer product were detected by autoradiographic exposure of the wet gel, and the extent of reaction at each time point was quantitated by scintillation counting of the excised gel slices. To determine the amount of covalent complex (E-17*/25-mer) present at each time point, a second 9-μL aliquot of each quenched sample was mixed with 9 μL of SDS sample buffer [15% 2-mercaptoethanol, 30% glycerol, 6% (w/v) SDS, 188 mM Tris (pH 6.8), 0.015% bromophenol blue] and applied to a 13% SDS–polyacrylamide gel. After electrophoresis, the sections corresponding to the radiolabeled covalent complex and free DNA were excised from the gel, and the radioactivity was determined by liquid scintillation spectrometry. The fraction of the total radioactivity present in each species (19*-mer, 25*-mer, and E–17*/25-mer) was calculated and then normalized by dividing by the fraction of 19-mer (0.60) that reacted at very long times [i.e., $\%_{norm}$ = [(frac X)$_t$/0.6] × 100, where frac X is the fraction of the total radioactivity present in each species at each time]. Computer simulation of the time courses was performed with the kinetic simulation program SIM87 (Stahl & Jencks, 1987).

Cleavage–Religation of 25/25-mer. The rate of covalent complex formation with the 5′-^{32}P-labeled 25*/25-mer duplex product (Figure 2C) and the internal equilibrium constant on the enzyme were determined by monitoring the single-turnover approach to equilibrium under conditions of excess enzyme such that all the duplex is enzyme bound. In this experiment a 40-μL solution consisting of 62 nM 25/25-mer and 36 μM 8-mer was mixed with 1 μM topoisomerase in 50 mM Tris-HCl, pH 7.5, at 20 °C in the rapid quench flow apparatus. A large excess of unlabeled 8-mer was included in the reaction to prevent dissociation of the 8-mer strand from the E–17*/25-mer 8-mer complex. Samples were quenched in 2% SDS delivered from the quench syringe at times ranging from 0.5 to 10 s. The radiolabeled E–17*/25-mer was resolved from free DNA by SDS–polyacrylamide gel electrophoresis as described above for the strand religation kinetic experiments. The radioactivity present in the complex and free DNA at each time was determined by liquid scintillation counting of the excised gel slices. The data are expressed as a percentage of the total radioactivity at each time trapped in the covalent complex (see above). The first-order rate constant for approach to equilibrium cleavage of the 25*/25-mer (k_{obsd}) was obtained from a nonlinear least-squares fit of the data to a single exponential. The cleavage (k_{cl}) and religation (k_r) rate constants were then calculated from k_{obsd} and the internal equilibrium constant for cleavage (K_{cl}) by the simultaneous solution of eqs 1 and 2.

Steady-State Cleavage–Religation Kinetics. Multiple-turnover reactions (20 or 40 μL) containing 50 mM Tris-HCl, pH 7.5, at 20 °C, 2–10 μM 3′-^{3}H- or 3′-^{32}P-labeled 19/25-mer and 18 μM complementary 8-mer in the presence or absence of 100 mM NaCl were initiated by the addition of topoisomerase to a final concentration of 50–500 nM. Under these limiting enzyme conditions, the enzyme is released from the covalent complex by the large excess of 8-mer to perform multiple cleavage–religation cycles. At time points between 4 and 300 s, reaction aliquots (5 μL) were removed and manually quenched in 5 μL of 2% SDS. After the pre-steady-state burst phase, the steady-state rate of dinucleotide release was obtained from the linear rate of appearance (with <6% conversion) of the radiolabeled dinucleotide product using the TLC assay described above. Since the enzyme is saturated with substrates under these conditions (V_{max}), the steady-state value for k_{cat} is obtained by dividing the velocity by the enzyme concentration. The burst and steady-state rates were analyzed as described (Fersht, 1985a).

DNA Binding Equilibria and Product Release Rates. A nitrocellulose filter binding assay (Riggs et al., 1970) was used to determine the noncovalent binding affinity of the topoisomerase for the 25/25-mer duplex. In this assay free duplex DNA will pass through the nitrocellulose filter while DNA bound to enzyme is retained on the membrane. Since the measurement of DNA–topoisomerase noncovalent binding affinity is complicated by the covalent reaction, the binding experiments were performed in the presence of a large excess of 8-mer single-strand DNA to prevent dissociation of the cleaved leaving strand. This is important because dissociation of the leaving strand would shift the internal equilibrium (K_{cl}) toward the cleaved covalent species, resulting in tighter apparent binding constants. The binding reactions (20 μL), which were incubated for 30 min at 20 °C in 50 mM Tris-HCl, pH 7.5, contained 0–140 nM topoisomerase and 15.6 nM 5′-^{32}P-labeled 25/25-mer duplex. Samples (9 μL) were applied to nitrocellulose (0.2-μm pore size, 25-mm diameter, Whatman) on a vacuum apparatus (Millipore) and aspirated. Filters were washed under vacuum with five 1-mL aliquots of wash buffer (50 mM Tris-HCl and 0.1 mM EDTA, pH 7.5), and the retained radioactivity was determined by liquid scintillation counting. Nine microliters of each reaction mixture was spotted on nitrocellulose without aspiration to determine the total counts in the reaction mix. The data were corrected for nonspecific binding of free DNA (≤12%), and the dissociation constant (K_D) was obtained from a nonlinear least-squares fit of the data to

$$[E]_{bound} = \frac{[E]_{free} C}{K_D + [E]_{free}} \quad (3)$$

where C is the total concentration of DNA duplex present.

Table 1: Kinetic and Thermodynamic Parameters of Vaccinia DNA Topoisomerase I at 20 °C, pH 7.5

parameter	units	method (weight)[a]	value	average
k_{cl}	s^{-1}	ST cleavage (1)[b]	0.06 ± 0.01	0.07 ± 0.01
		approach to eq. (3)	0.083 ± 0.014[c]	
		pre-SS burst (2)[d]	0.058 ± 0.013	
K_M^S	nM	ST cleavage (1)[b]	70 ± 20	70 ± 20
k_r	s^{-1}	ST religation (1)[b]	0.53 ± 0.09	0.66 ± 0.10
		approach to eq. (2)	0.73 ± 0.1	
K_{cl}		k_{cl}/k_r (1)	0.11 ± 0.02	0.12 ± 0.02
		approach to eq. (2)	0.13 ± 0.02[c]	
k_{off}^{prod}	s^{-1}	off rate (1)	0.010 ± 0.001	0.008 ± 0.001
		SS k_2 value (2)[d]	0.0074 ± 0.0014	
K_D^{prod}	nM	filter binding (1)	54 ± 6	54 ± 6
k_{on}^{DNA}	$M^{-1}\ s^{-1}$	ST (k_{cl}/K_M^S) (1)[b]	(8 ± 3) × 10^5	(5 ± 3) × 10^5
		k_{off}/K_D^{prod} (1)	(1.5 ± 0.2) × 10^5	
		$k_{cl}/(K_M^S - K_D^{prod})$ (1)	(5 ● 1) × 10^5 [e]	

[a] Weight based on number of experiments done (see text). [b] ST, single turnover. [c] Average of several values given in text. [d] SS, steady state. [e] Calculated for both substrate 19/25-mer and product 25/25-mer assuming $K_D^S = K_D^{prod}$.

Scheme 1

$$19^*/25\text{-mer} \underset{k_{-1}}{\overset{k_1[E]}{\rightleftharpoons}} E{\cdot}19^*/25\text{-mer} \xrightarrow{k_{cl}} E\text{–}17/25\text{-mer}{\cdot}dApT^*$$

The rate constant for 25/25-mer release from the enzyme in the presence and absence of 5 mM $MgCl_2$ was determined using the nitrocellulose filter binding method. A reaction mixture (50 μL) consisting of 25 nM 5′-^{32}P-labeled 25/25-mer, 3.7 μM 8-mer, and 326 nM topoisomerase in 50 mM Tris-HCl, pH 7.5, in the presence or absence of 5 mM $MgCl_2$ was preincubated for 10 min at 20 °C. The reaction was initiated by the addition of a large excess (1–2 μM) of unlabeled 25/25-mer, and at varying times 5-μL portions of the reaction mixture were removed and applied to the nitrocellulose filters (10 time points, 0–30 min). The filters were processed as described above for the equilibrium binding measurements, and the rate constants were determined from a nonlinear least-squares fit of the data to a single exponential. Under these conditions the observed rate constant represents that for product dissociation because trapping of the free enzyme was zero-order in the 25/25-mer trap.

Binding of Mn^{2+} to Topoisomerase. The binding of Mn^{2+} to the enzyme was determined by two independent techniques, electron paramagnetic resonance which measures free Mn^{2+} (Cohn & Townsend, 1954) and the enhancement of the longitudinal relaxation rate of water protons which measures an effect of bound Mn^{2+} (Mildvan & Cohn, 1963).

RESULTS

The structures of the 19/25 cleavage substrate, 8-mer ligation substrate, and 25/25-mer cleavage–ligation product are shown in Figure 2. The results of the kinetic experiments described below are summarized in Scheme 7 and Table 1.

Determination of k_{cl} and k_{cl}/K_M for 19/25-mer. The observed first-order rate constants for the irreversible reaction of topoisomerase (E) with the 3′-^{32}P-labeled 19/25-mer substrate (Scheme 1) were determined in single-turnover experiments with excess enzyme (500 nM) and limiting 19*/25-mer (2–75 nM) by following the appearance of the radiolabeled dinucleotide product (dApT*) by TLC (Figure 3). Under these conditions the reaction was zero-order in 19/25-mer and displayed saturable kinetics with respect to

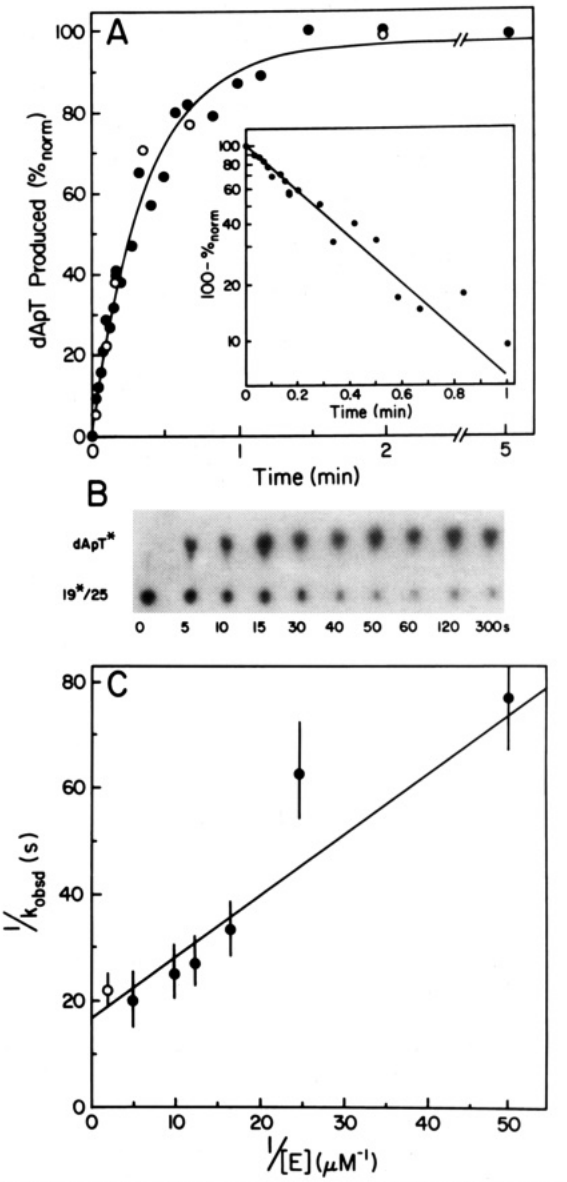

FIGURE 3: Single-turnover cleavage of 3′-^{32}P-labeled 19*/25-mer in 50 mM Tris-HCl, pH 7.5, and 20 °C. (A) Reactions contained 500 nM enzyme, 10 nM 3′-^{32}P-labeled 19*/25-mer in the absence (closed circles) and presence (open circles) of 5 mM $MgCl_2$. The percent ^{32}P-labeled dApT* produced at each time point was normalized ($\%_{norm}$) to the final observed end point of the reaction, as described under Materials and Methods. (B) Autoradiogram of cleavage reaction time points (0–300 s) analyzed by poly(ethylenimine)-cellulose thin-layer chromatography as described under Materials and Methods. (C) Dependence of the observed rate constant for cleavage on the topoisomerase concentration. Closed circles, reaction of 2 nM 19*/25-mer with 20–200 nM topoisomerase; the open circle represents the rate constant obtained from the data in panel A.

enzyme concentration (Figure 3C) according to

$$k_{obsd} = \frac{k_{cl}[E]}{K_m^S + [E]} \quad (4)$$

In eq 4, k_{cl} is the rate constant for cleavage extrapolated to infinite enzyme concentration and K_m^S is the Michaelis constant of the substrate, which has the form of

$$K_m^S = \frac{k_{-1} + k_{cl}}{k_1} \quad (5)$$

From the data of Figure 3C, $k_{cl} = 0.06 \pm 0.01\ s^{-1}$, $k_{cl}/K_m^S = (8 \pm 3) \times 10^5\ M^{-1}\ s^{-1}$, and $K_m^S = 70 \pm 20$ nM. In other experiments, the extent of dinucleotide release was found to

Scheme 2

$$\text{E–17}^*\text{/25-mer•8-mer} \underset{k_{cl}}{\overset{k_r}{\rightleftharpoons}} \text{E•25}^*\text{/25-mer}$$

be independent of the presence or absence of SDS, indicating that the detergent did not induce DNA strand cleavage.

The data of Figure 3A also show that the cleavage reaction is unaffected by the presence of 5 mM $MgCl_2$. This result demonstrates that the 3–10-fold rate increase observed for the relaxation of negatively supercoiled plasmid DNA in the presence of 5 mM $MgCl_2$ (Shaffer & Traktman, 1987; Shuman et al., 1988) is not a result of Mg^{2+} ion enhanced catalysis of the cleavage step. No significant Mn^{2+} binding to the enzyme was detected either by EPR or by the enhancement of the longitudinal water proton relaxation rate ($\epsilon^* \leq 1.5$), indicating that $K_D^{Mn2+} \geq 3$ mM.

It has previously been shown that mutation of the active site Tyr-274 to Phe (Y274F) abrogates enzymatic activity (Shuman et al., 1989b). The cleavage reaction of the Y274F mutant with the 19/25-mer substrate was investigated under single-turnover conditions. Although the mutant enzyme was saturated with the 19/25-mer as shown by parallel nitrocellulose filter binding studies under similar conditions, no dApT* cleavage product was detected. The upper limit value of $k_{cl} \leq 4.5 \times 10^{-8}$ s^{-1} obtained with this mutant supports the essential nature of this residue.

Rate of Strand Religation (k_r). The rate constant for approach to equilibrium ligation of the 8-mer strand to the preformed 5′-^{32}P-labeled covalent complex (E–17*/25-mer) was determined according to the reaction in Scheme 2 by following the disappearance of the E–17*/25-mer on an SDS–polyacrylamide gel as described under Materials and Methods. The 8-mer strand was present in large molar excess so that the rate of ligation was zero-order in 8-mer concentration over the range tested (8–18 μM). Under these conditions the observed rate constant (k_{obsd}) is equal to the sum of the forward rate constant for religation (k_r) and the reverse cleavage rate constant (k_{cl}) according to eq 1. Values for $k_r = 0.53 \pm 0.09$ s^{-1} and $k_{cl} = 0.09 \pm 0.02$ s^{-1} are calculated from the values of $k_{obsd} = 0.62 \pm 0.07$ s^{-1} and $K_{cl} = k_{cl}/k_r = 0.16 \pm 0.02$ obtained from the data in Figure 4; the calculated value of k_{cl} obtained here is within experimental error of the value of k_{cl} measured in the irreversible cleavage experiment (Table I).

Previous studies of intermolecular strand religation (Shuman, 1992), using similar duplex substrates as employed here demonstrated that (1) this reaction requires at least four base pairs between the incoming acceptor strand and the single strand overhang of the cleaved substrate, and (2) acceptor strands with complete sequence complementarity with the single-strand overhang were ligated more efficiently than strands forming base pair mismatches. It should be mentioned that intramolecular strand religation reactions with the 5′-OH group of the uncleaved strand have been observed; however, these reactions are significantly less favorable than the intermolecular reactions (Shuman, 1992). Consistent with this observation, no significant intramolecular strand religation was detected in this study, and identical results were achieved with substrates containing either 5′-OH or 5′-phosphoryl groups on the uncleaved strand (not shown).

Coupled Strand Cleavage–Religation. In the experiments shown in Figures 3 and 4 the rate constants, k_{cl} and k_r, for the isolated cleavage and religation partial reactions were determined. In the experiment shown in Figure 5, the cleavage and religation reactions between the 19/25-mer and 8-mer substrates are coupled in a single system to determine whether

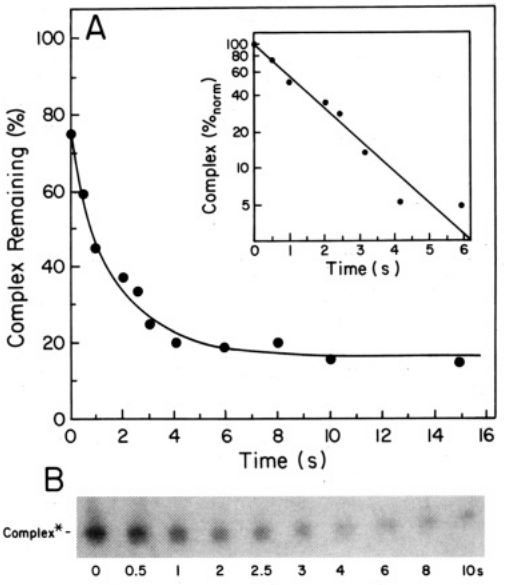

FIGURE 4: Determination of the rate of strand religation by single-turnover approach to equilibrium kinetics at pH 7.5, 20 °C. (A) 40 μL of 36 nM 5′-^{32}P-labeled covalent complex (E–17*/25-mer), which was formed by incubating 1 μM topoisomerase with 50 nM 5′-^{32}P-labeled 19*/25-mer for 15–30 min at room temperature, was mixed with 40 μL of 36 μM 8-mer in the rapid quench flow apparatus and quenched at the indicated times in 2% SDS. The radiolabeled E–17*/25-mer was resolved from free DNA by electrophoresis on a 13% SDS–polyacrylamide gel (panel B), and the percent of the total radioactivity present in E–17*/25-mer at each time was determined by liquid scintillation counting of the excised gel slice (see text). (Inset) Semilogarithmic plot of the data in panel A. In this replot, the data are presented as a percent of the initial amount of covalent complex remaining at each time (i.e., $\%_{norm}$ = (% complex)$_t$/(% complex)$_{t=0}$). (B) Autoradiogram of a 13% SDS–polyacrylamide gel showing the disappearance of the 5′-^{32}P-labeled E–17*/25-mer as a function of time.

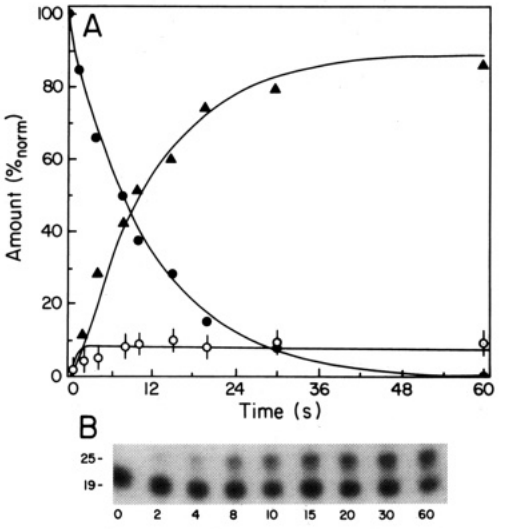

FIGURE 5: Coupled strand cleavage–religation in a single-turnover. (A) Reactions contained 25 nM 5′-^{32}P-labeled 19*/25-mer, 18 μM 8-mer, and 500 nM topoisomerase; time points were quenched in 1% SDS. The 5′-^{32}P-labeled 19*-mer strand (●) and 25*-mer ligation product (▲) were resolved by electrophoresis on a 19% polyacrylamide/7.5 M urea denaturing gel (panel B). After autoradiography the bands were excised, and the radioactivity was determined by liquid scintillation spectrometry. The radiolabeled E–17/25-mer (○) was resolved by SDS–polyacrylamide gel electrophoresis and quantitated as described in the legend to Figure 3, panel A. The lines are the computer simulated fits of the data to the model shown in Scheme 3 using values for $k_{cl} = 0.08$ s^{-1} and $k_r = 0.75$ s^{-1}.

Scheme 3

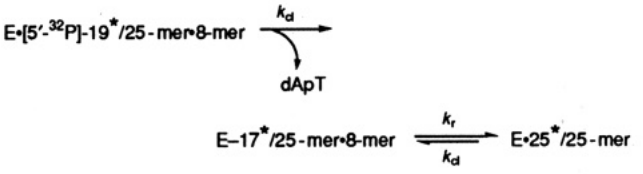

the independently determined values for k_{cl} and k_r adequately describe the kinetics for the coupled system.

The coupled strand cleavage–religation reaction was studied in a single-turnover experiment as described in Figure 5 with excess topoisomerase (500 nM) and 8-mer (18 μM) and limiting 5′-^{32}P-labeled 19/25-mer (25 nM) according to the reaction in Scheme 3. Under the conditions of this reaction, essentially all of the substrates are enzyme bound,[2] and therefore binding steps are not observed. Similarly, the equilibrium endpoint represents the internal equilibrium (K_{cl}) for cleavage of the enzyme bound 25/25-mer (E•25/25-mer) product.

As shown in Figure 5, as the substrate concentration decreases with time, the intermediate reaches a steady state, and the product appears and increases with time. The curves in Figure 5 were computed using the mechanism shown in Scheme 3 and the rate constants $k_{cl} = 0.08$ s^{-1} and $k_r = 0.75$ s^{-1}. These rate constants are in reasonable agreement with the values for $k_{cl} = 0.06 \pm 0.01$ and $k_r = 0.53 \pm 0.09$ determined from the isolated half-reactions and the rate constants for cleavage and religation of the 25/25-mer reported in Table 1. That the product of the religation reaction was indeed the 25-mer was confirmed by denaturing polyacrylamide gel electrophoresis of the DNA product (not shown).

Strand Cleavage and Noncovalent Binding of 25/25-mer. The cleavage reaction of the 25/25-mer duplex was studied to determine if the rate of cleavage is significantly different when the substrate is base-paired 3′ to the cleavage site. The rate and extent of covalent complex formation (E–17*/25-mer) starting from the 5′-^{32}P-labeled 25/25-mer was determined by a single-turnover approach to equilibrium kinetic experiment (Figure 6) in the presence of excess enzyme (500 nM) and limiting 25/25-mer (31 nM) according to the reaction in Scheme 4. Reactions were quenched in 1% SDS, and the radiolabeled E–17*/25-mer was resolved by SDS–polyacrylamide gel electrophoresis and quantitated as described in the legend to Figure 3A. Values for $k_{cl} = 0.078 \pm 0.012$ and $k_r = 0.70 \pm 0.1$ were calculated from the observed rate constant for approach to equilibrium $k_{obsd} = k_{cl} + k_r = 0.78 \pm 0.1$ s^{-1} and the equilibrium end point for the reaction $K_{cl} = k_{cl}/k_r = 0.11 \pm 0.01$. Thus, the rates of cleavage and religation of the 19/25-mer and 25/25-mer do not differ significantly.

The equilibrium dissociation constant (K_D^{prod}) for the 25/25-mer was determined by a nitrocellulose filter binding assay under conditions which minimize the contribution of the covalent complex to the total binding affinity. The binding experiment (Figure 7) was performed in the presence of a large excess of 8-mer (9 μM) to prevent dissociation of the cleaved leaving strand as shown in Scheme 5 and thus yields a true dissociation constant. Control experiments demonstrated that concentrations of 8-mer in the range 1–18 μM did not competitively inhibit ($\leq$5%) binding of the labeled

[2] It is not known whether the 8-mer strand is presented to the enzyme as a duplex, partially hybridized to the single-strand overhang of the 19/25-mer, or reacts directly with the E-17/25-mer complex. However, detailed knowledge of the mechanism is not required for interpretation of the data since the reaction is zero-order with respect to 8-mer.

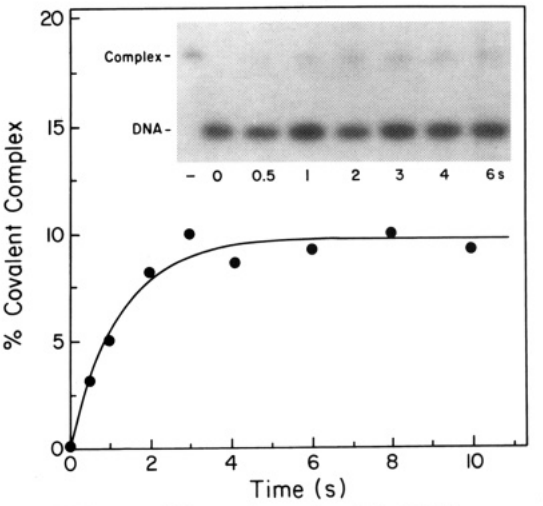

FIGURE 6: DNA strand cleavage reaction of the 25/25-mer product. Determination of the rate and extent of covalent complex formation (E–17*/25-mer) with the 5′-^{32}P-labeled 25*/25-mer product by single-turnover approach to equilibrium kinetics. Forty microliters of 62 nM 25*/25-mer and 40 μL of 1 μM topoisomerase in 50 mM Tris-HCl, pH 7.5, at 20 °C were mixed in the rapid quench flow apparatus and quenched in 2% SDS at times ranging from 0.5 to 10 s. The radiolabeled E–17*/25-mer was resolved by SDS–polyacrylamide gel electrophoresis (autoradiogram shown in inset) and quantitated as described in the legend to Figure 3, panel A. The line is the calculated fit of the data to a single exponential. The cleavage (k_{cl}) and religation (k_r) rate constants were calculated from the observed rate constant for approach to equilibrium ($k_{obsd} = k_{cl} + k_r = 0.78 \pm 0.1$ s^{-1}) and the measured equilibrium constant for the reaction ($K_{cl} = k_{cl}/k_r = 0.11$).

Scheme 4

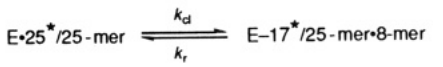

Scheme 5

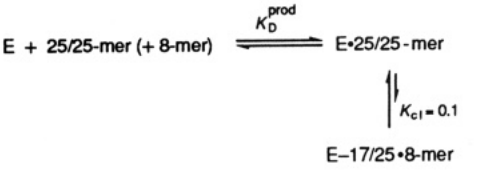

25/25-mer to the enzyme as judged by the nitrocellulose filter binding assay (not shown). This result is consistent with previous reports that the enzyme has no significant affinity for single-stranded DNA (Shuman, 1991a; Morham & Shuman, 1992). Therefore, since the internal cleavage equilibrium ($K_{cl} = 0.1$, Scheme 5) strongly favors the uncleaved duplex (E•25/25-mer) and the system is saturated with 8-mer, the value of $K_D^{prod} = 54 \pm 6$ nM obtained from the data in Figure 7 closely approximates the true equilibrium dissociation constant. The Scatchard analysis of the binding data (Figure 7, inset) gives a stoichiometry of one enzyme molecule bound per 25/25-mer duplex.

Determination of Steady-State k_{cat}. It is important when performing pre-steady-state kinetic measurements to confirm that the observed rates (i.e., k_{cl} and k_r) are consistent with the activity of the enzyme under steady-state conditions. Therefore, the cleavage–religation reactions were studied in multiple-turnover kinetic experiments with limiting enzyme and excess 3′-labeled 19/25-mer and 8-mer substrates as shown in Scheme 6.

Under the conditions of this experiment the enzyme is saturated with both substrates, and the steady-state rates were the same in the presence of 2–10 μM 19/25 mer and 1–18 μM

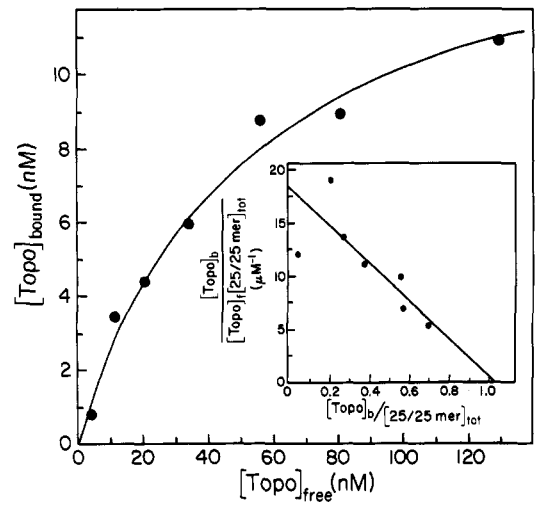

FIGURE 7: Determination of the dissociation constant (K_D^{prod}) and binding stoichiometry of the product (25/25-mer) as assayed by nitrocellulose filter binding. Reactions (in 50 mM Tris-HCl, pH 7.5) containing 15.6 nM 5′-^{32}P-labeled 25*/25-mer, 5–140 nM topoisomerase, and 9 μM 8-mer were incubated for 30 min at 20 °C and transferred to nitrocellulose under vacuum as described under Materials and Methods. The 8-mer strand was included to prevent dissociation of the 3′-portion of the cleaved strand; under these conditions the covalent enzyme–DNA species contributes only 10% to the total observed binding at each topoisomerase concentration (see text and legend to Figure 6). The solid line is the calculated fit of the data to eq 3. The inset shows a Scatchard analysis of the binding data.

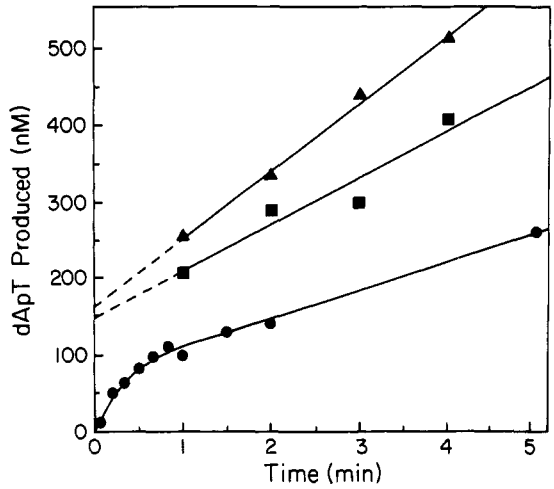

FIGURE 8: Multiple-turnover cleavage–religation kinetics. Reactions (50 mM Tris-HCl, 100 mM NaCl, pH 7.5, and 20 °C) contained 10 μM 3′-^{3}H-labeled 19*/25-mer, 18 μM 8-mer and either 90 nM (circles), 140 nM (squares), or 188 nM (triangles) topoisomerase. The best-fit lines for the reactions containing 140 and 188 nM topoisomerase are extrapolated to zero time to illustrate the burst amplitudes which are within experimental error of the values calculated from eq 7 (see text). The kinetics of the burst phase is shown for the reaction of 90 nM topoisomerase; the line is the nonlinear least-squares fit of the data to eq 6.

8-mer. The amount of radiolabeled dApT* produced at each time is given by eq 6,which is derived from the kinetic

$$[\text{dApT*}] = [E_0]\left[\frac{k_{cl}}{k_{cl}+k_2}\right]\left[\frac{k_{cl}}{k_{cl}+k_2}(1-\exp[-(k_{cl}+k_2)t]) + k_2 t\right] \quad (6)$$

mechanism in Scheme 6.

In Scheme 6, k_{cl} is the first-order rate constant for cleavage, and k_2 is the net forward rate constant in the steady state

Scheme 6

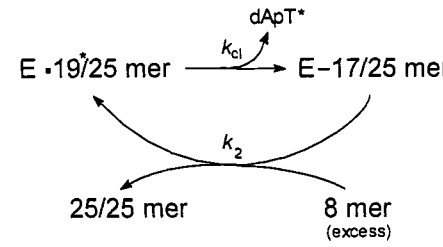

which includes all steps subsequent to cleavage (Cleland, 1975). In the limiting case, when $k_{cl} \gg k_2$ there will be an initial first-order burst of dApT* formation (k_{burst}) followed by a linear increase as the covalent intermediate (E–17/25-mer) turns over. In the other limiting case, when $k_2 \gg k_{cl}$, there is no burst and the observed linear rate is equal to k_{cl}. The expressions for the burst amplitude, linear rate (V_{max}), and k_{burst}, which are obtained from eq 6, are given by eqs 7–9 (Fersht, 1985).

$$\text{burst amplitude} = [E_0]\left(\frac{k_{cl}}{k_{cl}+k_2}\right)^2 \quad (7)$$

$$k_{burst} = k_{cl} + k_2 \quad (8)$$

$$V_{max} = [E_0]\frac{k_{cl}k_2}{k_{cl}+k_2} = [E_0]k_{cat} \quad (9)$$

The data shown in Figure 8 for the reaction of 90, 140, or 188 nM topoisomerase with 10 μM 3′-^{3}H-labeled 19/25-mer and 18 μM 8-mer clearly show an initial burst phase with amplitudes proportional to enzyme concentration. Subsequent to the burst, a linear phase is seen, the slope of which (V_{max}) is directly proportional to the enzyme concentration. A value for $k_{cat} = 0.006 \pm 0.0004$ s^{-1} was obtained from the slope of a plot of V_{max} against total enzyme concentration (not shown). From k_{cat} and k_{cl} determined from steady-state and single-turnover experiments, respectively, a value of $k_2 = 0.0067 \pm 0.0007$ s^{-1} is then obtained using eq 9. The observed burst amplitudes are within experimental error (±20%) of the values calculated from eq 7 using the experimentally determined values for k_{cl} and k_2. The nonlinear least-squares fit of the data for the reaction of 90 nM topoisomerase to eq 6 gave similar values of $k_{cl} = 0.045 \pm 0.01$ s^{-1} and $k_2 = 0.008 \pm 0.002$ s^{-1}, with $[E_0] = 77 \pm 10$ nM.

These results are consistent with a steady-state mechanism in which the chemical step (k_{cl}) is fast compared to a subsequent step with the rate constant k_2. Since the religation rate constant is ≈10-fold faster than k_{cl} (see above results), the small magnitude of k_2 can be reasonably attributed only to rate-limiting product release. This interpretation is further supported by direct measurement of the rates of product release from the enzyme as determined by the nitrocellulose filter binding assay (Figure 9). In the absence of $MgCl_2$ (Figure 9), a value of $k_{off}^{prod} = 0.01 \pm 0.001$ s^{-1} was obtained, which is not significantly different from the values of k_2 obtained in the steady-state system (Table 1). In the presence of 5 mM $MgCl_2$ (Figure 9) the dissociation rate constant is increased ~9-fold ($k_{off,Mg^{2+}}^{prod} = 0.094 \pm 0.015$ s^{-1}) providing an explanation for the Mg^{2+}-induced 3–10-fold increase in the rate of relaxation of negatively supercoiled DNA by this enzyme (Shaffer & Traktman, 1987; Shuman et al., 1988). A similar ≥15-fold increase in the equilibrium dissociation constant of the enzyme–DNA complex in the presence of 5 mM $MgCl_2$ has been observed (Shuman & Prescott, 1990). Further experiments (not shown) demonstrated that the k_{cat} value

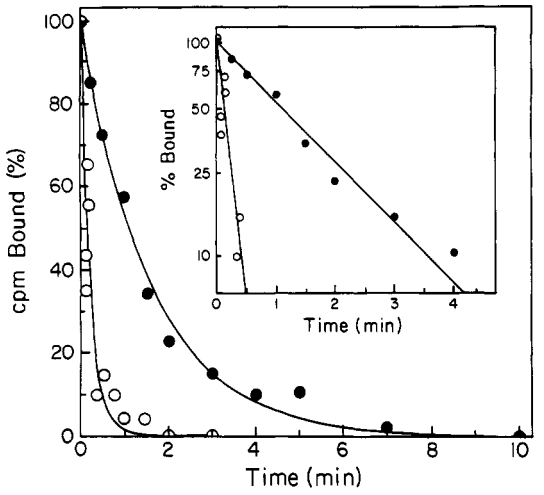

FIGURE 9: Rate of 25/25-mer release from topoisomerase in the presence (open circles) and absence (closed circles) of 5 mM $MgCl_2$ as determined by nitrocellulose filter binding. Reaction mixtures (±5 mM $MgCl_2$) containing 25 nM 5′-^{32}P-labeled 25/25-mer, 3.7 μM 8-mer, and 326 nM enzyme were preincubated for 10 min at 20 °C before the addition of a large excess (2 μM) of unlabeled 25/25-mer. Samples were removed at the indicated times, transferred to nitrocellulose filters, and aspirated. Plotted is the percent of the initial cpm which were bound to the membrane as a function of time after addition of excess unlabeled 25/25-mer. The lines are the calculated fits of the data to single exponentials. The inset shows the semilogarithmic plots.

Scheme 7

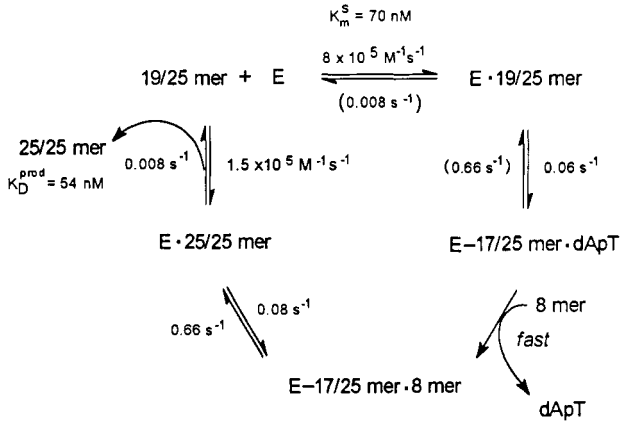

was the same in the presence of 0 or 100 mM NaCl and increased about 2-fold in the presence of 250 mM NaCl, consistent with a salt-induced increase in the rate of product release. The possibility that the small observed value of k_{cat} results from severe product inhibition is excluded by the observation that K_m^S for the 19/25-mer and K_D^{prod} are similar (see Scheme 7); additionally there is no decrease in slope in Figure 8 as 25/25-mer accumulates, as would be expected from severe product inhibition.

It is important to point out that the steady-state reaction is catalytic, with ≥22 turnovers at S/E ratios of 100:1, and ~90% of the substrate reacts at long times with [substrate]/[enzyme] ratios of 22:1 (not shown). Furthermore, catalytic turnover requires the presence of the 8-mer strand. Control experiments in which 190 nM enzyme was incubated with 100 μM 19*/25-mer substrate in the absence of 8-mer yielded one enzyme equivalent (±20%) of dApT* after a 5-min incubation, consistent with irreversible formation of the covalent complex in the absence of 8-mer.

It is concluded that the above results support the steady-state mechanism shown in Scheme 6 and that the rate constants for cleavage and religation determined in single-turnover experiments are consistent with the activity of the enzyme in the steady-state system.

Thio Effects on k_{cl} and k_{cat}. The substitution of a sulfur atom for a nonbridging oxygen atom of a phosphodiester to form a phosphorothioate linkage is expected to decrease the chemical reactivity of the phosphodiester to attack by nucleophiles by 4–11-fold on the basis of model studies (Herschlag et al., 1991). The absence of a rate decrease in an enzymatic reaction upon "thio substitution" can, with some limitations (Herschlag et al., 1991), provide evidence for a rate-limiting step other than covalent chemistry, such as substrate binding, product release, or a conformational change (Bryant & Benkovic, 1979; Mizrahi et al., 1985; McSwiggen & Cech, 1989; Griep et al., 1990; Patel et al., 1991; Wong et al., 1991). Additionally, thio substitution introduces a chiral center at phosphorus, and if there is a different rate for the two thio isomers, this would provide evidence for a specific contact of the enzyme with a phosphoryl oxygen (Eckstein, 1979).

The single-turnover cleavage reaction (see Scheme 1) between 500 nM enzyme and 80 nM 19/25-mer with a racemic phosphorothioate linkage at the attacked position is shown in Figure 10A. The data are markedly biphasic and are well fit to a double exponential: Ampl = 46 ± 5%; Amp2 = 54 ± 5%, k_{fast} = 0.010 ± 0.002 s^{-1}, and k_{slow} = 0.0004 s^{-1}. The same results were obtained using 15 nM thio-19/25-mer and 500 nM enzyme, indicating that the reaction is zero-order in substrate. The amplitudes of the two kinetic phases are nearly equal, within experimental error, suggesting that the two thio isomers have significantly different rates. The rate constants for the thio-substituted substrates correspond to thio effects (= $k_{cl}^{phos}/k_{cl}^{thio}$) of 4.6- and 115-fold when compared to the k_{cl}^{phos} = 0.046 s^{-1} for the reaction of 500 nM topoisomerase with 10 nM phosphodiester 19/25-mer (dashed line, inset in Figure 10A). The minimal conclusion from this experiment is that there is a thio effect of *at least* 4.6-fold on the single-turnover cleavage reaction, indicating that the chemical step is at least partially rate-limiting.

The steady-state reaction (Scheme 6) of 10 nM racemic phosphorothioate substituted 19/25-mer (5 μM each *R* and *S* isomers) and 18 μM 8-mer with 180 nM topoisomerase is shown in Figure 10B (solid circles). In comparison with the phosphodiester substrate (Figure 8), the thio-substituted 19/25-mer (Figure 10B) showed a smaller burst amplitude, consistent with a decrease in k_{cl} (eq 6), and a steady-state rate indistinguishable from that of the phosphodiester substrate, suggesting rate-limiting product dissociation. The data of Figure 10B were fitted to eq 6 assuming k_{cl} = 0.010 s^{-1} as found by the single-turnover experiment, taking into account that half of the enzyme was saturated with the less reactive thio isomer. The resulting value of k_2 = 0.006 ± 0.001 s^{-1}, which represents all steps subsequent to cleavage, is indistinguishable, within experimental error, from that found for the phosphodiester substrate, 0.0067 ± 0.0007 s^{-1}. The lack of a thio effect on k_2 (k_2^{phos}/k_2^{thio} = 1.1 ± 0.2) indicates that this step does not involve covalent chemistry and likely represents product dissociation.

DISCUSSION

A detailed description of the kinetic mechanism of type I topoisomerases has previously been elusive, because of the low sequence specificity of these enzymes for cleavage of DNA substrates and the resulting experimental difficulty of separately studying the partial reactions of DNA strand cleavage

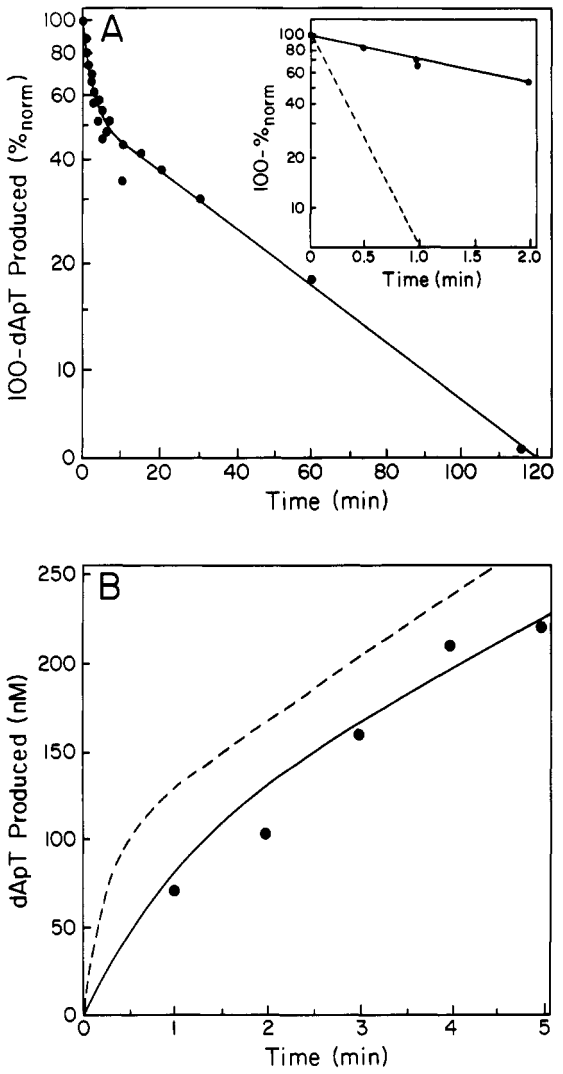

FIGURE 10: Thio effect on single-turnover and steady-state strand cleavage. (A) Single-turnover reaction of 500 nM topoisomerase with 83 nM racemic 3′-^{32}P-labeled 19^{thio*}/25-mer in 50 mM Tris-HCl, pH 7.5, at 20 °C. The percent dApT* produced at each time point was normalized ($\%_{norm}$) to the final observed end point of the reaction (55%) as described under Materials and Methods. A semilogarithmic plot of the data is shown, and the line is the nonlinear least-squares fit of the data to a double exponential. The inset shows an expansion of the early portion of the reaction. For comparison, the theoretical curve ($k_{cl} = 0.045\ s^{-1}$) for cleavage of the phosphodiester 19/25-mer by 500 nM topoisomerase is shown (dashed line). (B) Multiple-turnover cleavage–religation of the racemic 3′-^{32}P-labeled 19^{thio*}/25-mer substrate. Reaction containing 10 μM 19^{thio*}/25-mer (5 μM each *R* and *S* isomer), 18 μM 8-mer, and 180 nM topoisomerase in 50 mM Tris-HCl, pH 7.5, at 20 °C. The solid line was calculated using eq 6 and the rate constant for the faster reacting thio isomer as described in the text.

and religation. The type I topoisomerase from Vaccinia catalyzes a sequence-specific DNA strand cleavage–religation reaction with short linear DNA duplexes which has allowed a quantitative description of the kinetic mechanism of this enzyme. Table 1 summarizes the measured rate and equilibrium constants, and Scheme 7 shows the kinetic mechanism using the rate constants measured for each step. In parentheses in Scheme 7 are shown those rate constants which were obtained indirectly. The k_{on} of the product was calculated from its equilibrium dissociation constant and the rate constant for its dissociation. The religation and dissociation rate constants for the 19/25-mer substrate are reasonably assumed to be equal to those measured for the 25/25-mer product (*vide infra*).

The enzyme initially binds the 19/25-mer cleavage substrate with an apparent second-order rate constant $k_{cl}/K_m^S = 8 \times 10^5\ M^{-1}\ s^{-1}$ and an apparent affinity $K_m^S = 70$ nM. After formation of the binary E·19/25-mer complex, cleavage occurs with $k_{cl} = 0.06\ s^{-1}$. Following cleavage, the covalent E–17/25-mer complex is rapidly religated ($k_r = 0.66\ s^{-1}$) to the incoming 8-mer strand to form the enzyme-bound product 25/25-mer. Finally, the tightly bound product ($K_D^{prod} = 54$ nM) is slowly released from the enzyme with a rate constant $k_{off}^{prod} = k_2 = 0.008\ s^{-1}$ to complete a catalytic cycle. Omitted from Scheme 7 is the DNA topoisomerization step which, of course, cannot be studied in the linear substrates we have used. With supercoiled plasmids, the release of supercoils occurs in the cleaved, covalent enzyme–DNA complex at an estimated rate comparable to our measured rate of DNA strand religation (Shuman et al., 1988).[3]

The relative magnitudes of the rate constants for cleavage, religation, and product release ($k_{cl}/k_r \approx 0.1$, $k_{cl}/k_{off}^{prod} \approx 13$) show that the predominant enzyme species is the E·25/25-mer under steady-state k_{cat} conditions. The conclusion that the internal cleavage equilibrium (K_{cl}) on the enzyme favors the uncleaved complex by about 10-fold is consistent with a previous estimate of $K_{cl} = 0.16$ at 37 °C obtained from measurements of the amount of enzyme-bound *Nde*I-cut pUC19 DNA retained on a nitrocellulose filter in the presence and absence of 1% SDS (Shuman, 1991a; Shuman & Prescott, 1990). It is also consistent with the equilibrium point predicted on the basis of the free energy difference (1 kcal/mol) between tyrosine and ribose phosphodiesters (Champoux, 1990). The consistency of these results suggests that a cleavage equilibrium strongly favoring the uncleaved complex is a general feature of this type of reaction and is not unique to the duplexes used in this study. The implications of this result with respect to catalysis of relaxation of supercoiled substrates is discussed later.

Rate-Limiting Steps. The substantial thio effect of 4.6-fold in the single-turnover cleavage reaction, under conditions where the enzyme is largely saturated with substrate, is consistent with a rate-limiting bond breaking event under these conditions and provides no evidence for a kinetically significant conformational change before the cleavage step. This thio effect is within the range of values of 4–11-fold observed for the nonenzymatic nucleophilic substitution reactions of methyl-2,4-dinitrophenyl phosphate monoanion by several oxygen and amine-containing nucleophiles (Herschlag et al., 1991), suggesting that this effect is due to a slowing of the intrinsic chemical reactivity of the phosphodiester by sulfur.

The larger thio effect of 115-fold, which comprised 50% of the observed amplitude in the single-turnover experiment, suggests that the enzyme prefers a particular thio isomer. Assuming this interpretation, the Vaccinia enzyme discriminates against the more slowly reacting isomer by a factor of 25-fold, which is considerably less than the thio isomer discrimination of 500–1000-fold reported for snake venom phosphodiesterase and the ribozyme from *Tetrahymena* (Burgers & Eckstein, 1979; Herschlag et al., 1991). Presumably much of the discrimination seen for the phosphodiesterase and the ribozyme is due to the preference of the Mg^{2+} cofactor to coordinate only to oxygen in a phosphorothioate (Eckstein, 1979). The Vaccinia enzyme, which

[3] If the mechanism of supercoil release involves DNA rotation rather than DNA strand passage, the similarity of the rates of religation and supercoil release would provide a kinetic mechanism for the accumulation of topological isomers differing in linking numbers by steps of one (Champoux, 1990).

shows discrimination in the absence of a metal ion, may select one isomer by positioning a positively charged group in the active site, with only one of the thio isomers fulfilling the correct spatial requirements for catalysis.

The negligible thio effect on the steady-state rate, as well as the values of k_2 and k_{off}^{prod}, which agree and are approximately 10- and 100-fold less than the respective rate constants for cleavage and religation, provide confirmatory evidence for a rate-limiting product release step that limits turnover in the steady state. Rate-limiting product release under steady-state conditions is not uncommon for catalysts which bind oligonucleotide substrates and products with nanomolar affinities; product release is rate-limiting for Klenow DNA polymerase (Kuchta et al., 1987) and the GA_5 product of the L-21 *Sca*I ribozyme from *Tetrahymena* (Herschlag & Cech, 1990). As has been previously pointed out, such catalysts have not evolved for the facile release of product (Herschlag & Cech, 1990); in the case of topoisomerase, the slow turnover rate from the high-affinity site is consistent with a processive mechanism for relaxation at low salt concentrations (McConaughty et al., 1981).

The apparent second-order rate constant $k_{cl}/K_m^S = 8 \times 10^5$ M^{-1} s^{-1} for formation of the E–17/25-mer is far below the diffusion-controlled limit of 10^9 M^{-1} s^{-1} for the encounter of small molecules in aqueous solution (Eigen & Hammes, 1963) but approaches the range of values between 10^6 and 10^8 M^{-1} s^{-1} for binding of substrates to enzymes (Hammes, 1982). A direct measurement of the rate constant (or equilibrium constant) for binding of the 19/25-mer is not feasible due to the irreversibility of the cleavage reaction when the leaving group is only a dinucleotide. The most likely interpretation is that k_{cl}/K_m^S reflects the true second-order rate constant for substrate binding, which is supported by the small magnitude of the rate constant for product release in the steady state (i.e., $k_2 = 0.008$ s^{-1}). Since substrate resembles product, the off rate for the substrate is probably much slower than the rate of cleavage, so that the transition state for substrate binding is fully rate-limiting at subsaturating substrate. The reasons for low rates of substrate binding to enzymes have been discussed in detail elsewhere (Herschlag & Cech, 1990) and include limited accessibility of the active site (Schmitz & Schurr, 1972; McCammon & Northrup, 1981), requirements for desolvation of the active site and substrate (Bartlett & Marlowe, 1987; Holden et al., 1987), and multiple binding steps involving conformational changes in the enzyme or substrate (Burgen et al., 1975).

The assumption that the rate constants for substrate and product release are similar despite the presence of six extra nucleotides in the product is supported by the observation that 3′ segments of the scissile strand, 2–6 nucleotides in length, readily dissociate from the enzyme after the cleavage event (Shuman, 1991a). This implies that the enzyme does not interact strongly in the ground state with the leaving group of the cleaved substrate when it is small. Moreover, the similar values of k_{cl} obtained with the 19/25-mer and 25/25-mer substrates argue against a significant additional interaction of the enzyme with the 25/25-mer which lowers the kinetic barrier to cleavage. Consistent with this interpretation, there is no sequence conservation in this region between different cleavage sites in large plasmid substrates (Shuman & Prescott, 1990) and as few as two duplex nucleotides 3′ of the cleavage site are sufficient for cleavage (Shuman, 1992).

Catalytic Power of Vaccinia Topoisomerase. The average rate constants $k_{cl} = 0.07$ s^{-1} and $k_r = 0.66$ s^{-1} for the nucleophilic attack of Tyr-274 and deoxyribose 5′-OH at phosphorus (Table 1) represent $\sim 10^9$- and 10^{12}-fold rate enhancements, respectively, over the estimated rates of nucleophilic substitution at the phosphorus backbone of DNA at pH 7.5 by phenolate and alcoholate anions. The solution rates of $k_{PhO^-} = 2 \times 10^{-11}$ s^{-1} and $k_{R-O^-} = 3 \times 10^{-13}$ s^{-1} at pH 7.5 were estimated from the second-order rate constants for the reaction of phenolate and alcoholate anions with methyl-2,4-dinitrophenyl phosphate monoanion at 39 °C ($k_{PhO^-} = 3 \times 10^{-5}$ M^{-1} s^{-1}, $k_{R-O^-} = 4 \times 10^{-4}$ M^{-1} s^{-1}; Kirby & Younas, 1970), by adjusting for both the concentration of the nucleophilic anion form at pH 7.5 using the Henderson–Hasselbalch equation ($pK_{PhOH} \approx 10$, $pK_{ROH} \approx 15$) and the dependence of the reaction rate on the pK_a of the leaving group according to eq 10 (Kirby & Younas, 1970).

$$k_x = (k_{obsd}^{pH\ 7.5})10\ \exp[(\beta_{lg})(pK_x - pK_{DNP})] \qquad (10)$$

In eq 10, pK_x and pK_{DNP} are the pK_a values for the phenyl, alkyl, or 2,4-dinitrophenyl hydroxyl groups, respectively, and $\beta_{lg} = \delta(\log k)/\delta pK_{lg} \approx -1$ is the proportionality constant which relates the observed rate to the stability of the leaving group. The rate decrease observed for the Y274F mutant of at least 10^6-fold below that of the wild-type enzyme is consistent with these rate enhancement estimates.

These rate enhancements of 10^9–10^{12}-fold are considerably less than the rate acceleration of $\sim 10^{16}$-fold for attack of water at the phosphodiester backbone of DNA seen with staphylococcal nuclease and snake venom phosphodiesterase (Serpersu et al., 1987; Mildvan, 1992) but are similar to the rate enhancements of 10^8 and 10^{11}-fold reported for the *Sca*I ribozyme catalyzed cleavage of RNA by water and the ribose hydroxyl group of guanosine, respectively (Herschlag & Cech, 1990). Much of the catalytic power of these divalent cation-requiring catalysts can be directly attributed to the metal ion; coordination of the metal to a phosphoryl oxygen of the substrate can provide a large rate enhancement on the order of 10^4-fold (Herschlag & Jencks, 1990), and metal-bound hydroxyl groups are potent nucleophiles at neutral pH (Chaffee et al., 1973). The Vaccinia enzyme may provide similar catalysis in the absence of a metal by stabilizing the developing negative charge on the leaving group by juxtaposition of a cationic residue near the cleaved bond, lowering the pK_a of the attacking nucleophile, or providing general acid–base catalysis in the transition state for cleavage and religation.

Implications for Relaxation of Supercoiled Substrates. The values of k_{cl}, k_r, and k_{cat} reported here for the Vaccinia topoisomerase catalyzed cleavage of a linear duplex DNA substrate may be compared with the overall rates of relaxation of supercoiled plasmid DNA previously reported to provide insight into which of the individual steps in relaxation (i.e., cleavage, supercoil release, religation, or product release) might be rate-limiting under a particular set of reaction conditions.

The value of $k_{cl} = 0.06$ s^{-1} reported here is similar to the overall rate constant for relaxation of supercoiled plasmid DNA $k_{relax} = 0.035$ s^{-1}, which was obtained under single-turnover (processive) conditions at 20 °C and pH 7.9 with several eukaryotic type I topoisomerases (Caserta et al., 1990). The similar magnitudes of k_{cl} and k_{relax} suggest that DNA cleavage is overall rate-limiting under single-turnover conditions when product release is not observed. Under steady-state V_{max} conditions, with limiting enzyme and at low-salt ($\leq$10 mM), the estimated value of k_{relax} is about 10-fold slower than k_{cl} (Shaffer & Traktman, 1987), suggesting a different rate-limiting step than that observed under single-turnover conditions. Our comparable values of k_{cat} (0.006 s^{-1}) and of k_{off}^{prod} (0.010 s^{-1}), which are an order of magnitude slower than

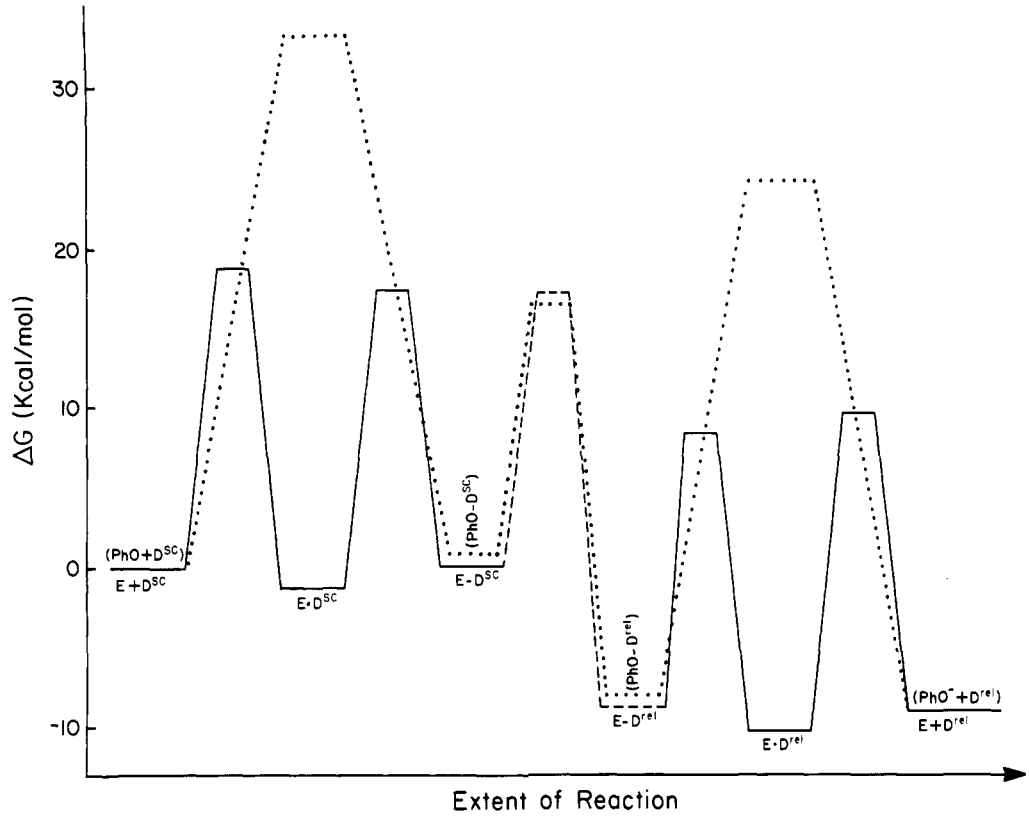

FIGURE 11: Free energy diagram of the reaction catalyzed by Vaccinia topoisomerase I. The profile for the enzyme (E)-catalyzed reaction (solid line) was constructed from the rate constants in Scheme 7 which were obtained at pH 7.5 and 20 °C and the estimated rate of topoisomerase catalyzed supercoil release (dashed, see text). For comparison, the estimated free energy profile for the uncatalyzed attack of phenolate anion (PhO^-) on supercoiled DNA (D^{sc}) at pH 7.5 and 39 °C is shown (dotted), based on model reactions with small phosphodiesters in solution and the spontaneous rate of relaxation of supercoiled DNA (see text). Apparent free energies of activation were calculated from $\Delta G^{act} = -RT \ln [k_{obsd}(h/k_BT)]$ using a standard state of 50 nM DNA cleavage sites. ΔG^{act} for intramolecular attack of the ribose 5′-OH group on the phosphophenol adduct (PhO–DNA) was estimated from the rate constant for attack of phenolate anion on phosphodiesters (see text) and the equilibrium free energy difference (1 kcal/mol) between tyrosine and ribose phosphodiesters (Champoux, 1990). The free energy of relaxed DNA (D^{rel}) is placed 9 kcal below that of supercoiled DNA (D^{sc}) (Gellert, 1983). Noncovalent and covalent interactions of the enzyme with the DNA are indicated as E·D and E–D, respectively.

the single-turnover strand cleavage rate (0.07 s^{-1}), indicate that the same step (i.e., product release) limits the steady-state rate of DNA relaxation and steady-state turnover in our system. The overall conclusion that strand cleavage and product release limit the rate of relaxation of supercoiled DNA under single-turnover and steady-state conditions, respectively, is consistent with the 10-fold faster rate constant for strand religation relative to cleavage reported here and with previous estimates of the relatively fast rate of DNA relaxation of 1–2 superhelical turns/s (Shuman et al., 1988; Caserta et al., 1990)[4] indicating that these steps are not rate-limiting.

Do type I topoisomerases catalyze the rate of supercoil release? The spontaneous rate of loss of supercoils from a plasmid has been estimated indirectly to be ≥10 s^{-1} with no detectable supercoiled intermediates at pH 7.5 and 30 °C following the nicking of a supercoiled plasmid at a single site with a restriction enzyme.[5] This rate is 5–10-fold greater than the estimated rate of the corresponding topoisomerase-catalyzed supercoil relaxation of ≥1–2 s^{-1} during which topological intermediates are detected (Shuman et al., 1988; Caserta et al., 1990). Hence topoisomerases, like that of Vaccinia, need not enhance the rate of supercoil release. On the contrary, topoisomerases may actually hinder the rate of supercoil release in order to control this process.[3]

The divalent cations Mg^{2+}, Mn^{2+}, Ca^{2+}, and Co^{2+} stimulate the relaxation of supercoiled plasmid DNA ~10-fold under steady-state conditions (Shaffer & Traktman, 1987; Shuman et al., 1988). The absence of an effect of 5 mM $MgCl_2$ on the rate of strand cleavage of the 19/25-mer substrate (Figure 3A) excludes a mechanism of activation involving direct metal ion assistance of this step. To increase the overall rate of relaxation, the metal ion must, at the very least, decrease the free energy barrier for the rate-limiting step. The present results establish product release to be the rate-limiting step under steady-state conditions at low salt, in accord with previous suggestions (McConaughty et al., 1981; Shuman et al., 1988; Shuman & Prescott, 1990), and demonstrate directly that Mg^{2+} accelerates this step by an order of magnitude, quantitatively explaining the Mg^{2+} stimulation of DNA supercoil relaxation. Consistent with this, $MgCl_2$ (5 mM)

[4] The estimated value of 1 superhelical turn/s at 20 °C was calculated from the value of k_{relax} = 0.035 s^{-1} (Caserta et al., 1990) and the total number of superhelical turns (ΔL = –30) initially present in the plasmid substrate [i.e., (0.035 s^{-1})(30 superhelical turns) = 1 superhelical turn/s].

[5] This experiment was performed by rapidly mixing a complex of lambda O protein and pRLM4 supercoiled DNA (ΔL = –38) with *Bam*H1 restriction enzyme and testing for residual supercoils by probing for O protein protection of an AT-rich region in the DNA against P1 nuclease digestion. O protein protection of this region requires that at least 33 negative supercoils be present in the DNA. The results of these experiments showed that at least five superhelical turns were removed from ≥50% of the supercoiled plasmids in 0.33 s. Thus, the lower limit for the spontaneous rate of supercoil release (0.693/0.33 s) × 5 superhelical turns is ≥10 superhelical turns s^{-1} (L. Huang, D. S. Sampath, and R. McMacken, personal communication, 1993).

decreases the affinity of the enzyme for DNA by a factor of ≥15-fold (Shuman & Prescott, 1990). The Mn^{2+} binding studies performed here exclude the possibility of a metal ion binding site on the free enzyme ($K_D \geq 3$ mM). Since DNA is known to bind divalent cations (Slater et al., 1972; Saenger, 1984), the activating effect of Mg^{2+}, Mn^{2+}, Ca^{2+}, and Co^{2+} on the overall rate of DNA relaxation is likely mediated through an effect of DNA-bound metal ions on the noncovalent interactions of DNA with the enzyme to facilitate release of the relaxed product.

The availability of the individual rate constants of Scheme 7 permits the construction of a free energy diagram of the overall topoisomerase reaction (Figure 11). This diagram illustrates the slow and tight binding of substrate, the unfavorable internal equilibrium for cleaved ($E\text{–}D^{sc}$) versus uncleaved enzyme-bound DNA ($E\cdot D^{sc}$), the rapid relaxation and religation of the cleaved DNA, and the rate-limiting dissociation of the product (D^{rel}). For comparison, the hypothetical free energy diagram of the uncatalyzed attack of phenoxide ion on DNA is shown, based on model reactions with small phosphodiesters in solution (Kirby & Younas, 1970) and on the spontaneous rate of relaxation of supercoiled DNA.[5] While the uncatalyzed reaction shows much higher barriers to DNA cleavage and religation than those found with the enzyme, the barrier to relaxation of cleaved DNA may actually be higher on the enzyme.

ACKNOWLEDGMENTS

We are grateful to Michael Washabaugh for the use of the rapid quench apparatus, to Ken Johnson for his advice on its operation, to Roger McMacken for permitting us to quote his unpublished data on the spontaneous relaxation of supercoiled DNA, and to Peggy Ford for secretarial assistance.

REFERENCES

Bartlett, P. A., & Marlowe, C. K. (1987) *Biochemistry 26*, 8553–8561.
Bryant, F. R., & Benkovic, S. J. (1979) *Biochemistry 18*, 2825–2828.
Burgen, A. S. V., Roberts, G. C. K., & Feeney, J. (1975) *Nature 253*, 753–755.
Burgers, P. M. J., & Eckstein, F. (1979) *Biochemistry 18*, 592–596.
Caserta, M., Amadei, A., Camilloni, G., & DiMauro, E. (1990) *Biochemistry 29*, 8152–8157.
Chaffee, E., Dasgupta, T. P., & Harris, G. M. (1973) *J. Am. Chem. Soc. 95*, 4169–4173.
Champoux, J. J. (1990) in *DNA Topology and its Biological Effects* (Cozzarelli, N. R., & Wang, J. C., Eds.) pp 217–242, Cold Spring Harbor Laboratory Press, Cold Spring Harbor, NY.
Cleland, W. W. (1975) *Biochemistry 14*, 3220–3224.
Cohn, M., & Townsend, J. (1954) *Nature 173*, 1090–1091.
Eckstein, F. (1979) *Acc. Chem. Res. 12*, 204–210.
Eigen, M., & Hammes, G. G. (1963) *Adv. Enzymol. Relat. Areas Mol. Biol. 25*, 1–38.
Fersht, A. R. (1985) *Enzyme Structure and Mechanism*, 2nd ed., pp 143–144, W. H. Freeman & Co., New York.
Gellert, M. (1981) *Annu. Rev. Biochem. 50*, 879–910.
Griep, M. A., Reems, J. A., Franden, M. A., & McHenry, C. S. (1990) *Biochemistry 29*, 9006–9014.
Hammes, G. G. (1982) *Enzymatic Catalysis and Regulation*, pp 99–101, Academic Press, New York.
Herschlag, D., & Cech, T. R. (1990) *Biochemistry 29*, 10159–10171.
Herschlag, D., & Jencks, W. P. (1990) *Biochemistry 29*, 5172–5179.
Herschlag, D., Piccirilli, J. A., & Cech, T. R. (1991) *Biochemistry 30*, 4844–4854.
Holden, H. M., Tronrud, D. E., Monzingo, A. F., Weaver, L. H., & Mathews, B. W. (1987) *Biochemistry 26*, 8543–8553.
Jencks, W. P. (1969) *Catalysis in Chemistry and Enzymology*, 1st ed., pp 586–589, McGraw Hill, New York.
Johnson, K. A. (1986) *Methods Enzymol. 134*, 677–705.
Kirby, A. J., & Younas, M. (1970) *J. Chem. Soc. B*, 1165–1172.
Kornberg, A., & Baker, T. A. (1992) *DNA Replication* (2nd ed.) pp 379–401, W. H. Freeman, New York.
Kuchta, R. D., Mizrahi, V., Benkovic, P. A., Johnson, K. A., & Benkovic, S. J. (1987) *Biochemistry 26*, 8410–8417.
Lee, M. P., Brown, S. D., Chen, A., & Shieh, T. (1993) *Proc. Natl. Acad. Sci. U.S.A. 90*, 6656–6660.
Maniatis, T., Fritsch, E. I., & Sambrook, J. (1982) *Molecular Cloning. A Laboratory Manual*, Cold Spring Harbor Laboratory, Cold Spring Harbor, NY.
McCammon, J. A., & Northrup, S. H. (1981) *Nature 293*, 316–317.
McConaughty, B. L., Young, L. S., & Champoux, J. J. (1981) *Biochim. Biophys. Acta 655*, 1–8.
McSwiggen, J. A., & Cech, T. R. (1989) *Science 244*, 679–683.
Mildvan, A. S. (1992) *FASEB J. 6*, A266, Abstract 1537.
Mildvan, A. S., & Cohn, M. (1963) *Biochemistry 2*, 910–919.
Mizrahi, V., Henrie, R. N., Marlier, J. F., Johnson, K. A., & Benkovic, S. J. (1985) *Biochemistry 24*, 4010–4018.
Morham, S. G., & Shuman, S. (1992) *J. Biol. Chem. 267*, 15984–15992.
Patel, S. S., Wong, I., & Johnson, K. A. (1991) *Biochemistry 30*, 511–525.
Riggs, A. D., Suzuki, H., & Bourgeois, S. (1970) *J. Mol. Biol. 48*, 67–83.
Saenger, W. (1984) *Principles of Nucleic Acid Structure*, pp 201–219, Springer-Verlag, New York.
Schmitz, K. S., & Schurr, J. M. (1972) *J. Phys. Chem. 76*, 534–545.
Serpersu, E. H., Shortle, D., & Mildvan, A. S. (1987) *Biochemistry 26*, 1289–1300.
Shaffer, R., & Traktman, P. (1987) *J. Biol. Chem. 262*, 9309–9315.
Shuman, S. (1989) *Proc. Natl. Acad. Sci. U.S.A. 86*, 3489–3493.
Shuman, S. (1991a) *J. Biol. Chem. 266*, 1796–1803.
Shuman, S. (1991b) *Proc. Natl. Acad. Sci. U.S.A. 88*, 10104–10108.
Shuman, S. (1992) *J. Biol. Chem. 267*, 8620–8627.
Shuman, S., & Moss, B. (1987) *Proc. Natl. Acad. Sci. U.S.A. 84*, 7478–7482.
Shuman, S., & Prescott, J. (1990) *J. Biol. Chem. 265*, 17826–17836.
Shuman, S., Golder, M., & Moss, B. (1988) *J. Biol. Chem. 263*, 16401–16407.
Shuman, S., Golder, M., & Moss, B. (1989a) *Virology 170*, 302–306.
Shuman, S., Kane, E. M., & Morham, S. G. (1989b) *Proc. Natl. Acad. Sci. U.S.A. 86*, 9793–9796.
Slater, J. P.; Tamir, I.; Loeb, L. A., & Mildvan, A. S. (1972) *J. Biol. Chem. 247*, 6784–6794.
Stahl, N., & Jencks, W. P. (1987) *Biochemistry 26*, 7654–7667.
Wang, J. C. (1985) *Annu. Rev. Biochem. 54*, 665–697.
Wong, I., Patel, S. S., & Johnson, K. A. (1991) *Biochemistry 30*, 526–537.